© Universiti Tun Hussein Onn Malaysia Publisher's Office

IJIE

http://penerbit.uthm.edu.my/ojs/index.php/ijie
ISSN : 2229-838X e-ISSN : 2600-7916

The International Journal of Integrated Engineering

CFD Simulation of Air-Piloted Downdraft Gasification Process: A Comparative Study Between Coal and Palm Kernel Shell as Feedstock

Mohd Amirul Mukminin Mohd Dali[1], Razlin Abd Rashid[1,2], Izuan Amin Ishak[1], Zuliazura Mohd Salleh[1,2], Rais Hanizam bin Madon[1,2], Mohammad Zulfikar Ishak[3], Nor Afzanizam Samiran[1,2]*

[1]Faculty of Engineering Technology,
Universiti Tun Hussein Onn Malaysia, Pagoh Higher Education Hub, 84600 Pagoh, Muar, Johor, MALAYSIA

[2]Integrated Engineering Simulation and Design (IESD) Focus Group,
Universiti Tun Hussein Onn Malaysia, Pagoh Higher Education Hub, 84600 Pagoh, Muar, Johor, MALAYSIA

[3]Els Energy and Lab Solutions Sdn Bhd,
No.11A Tingkat Merpati Dua, Taman Transkrian 14300 Nibong Tebal, Pulau Pinang, MALAYSIA

*Corresponding Author

DOI: https://doi.org/10.30880/ijie.2023.15.04.010
Received 21 December 2021; Accepted 11 January 2023; Available online 28 August 2023

Abstract: A fixed bed downdraft gasifier model based on computational fluid dynamic (CFD) framework was developed to investigate the influence of feedstock (palm kernel shell [PKS] and coal) on the quality of syngas produced via the gasification process. Euler–Euler approach was utilized in this study to describe the gas and solid phases. Realizable k-ε turbulence model was used to evaluate the constitutive properties of the dispersed phase and the gas phase behavior. This simulation model was validated by comparing the syngas composition of gasification simulation of coal with previous research, which yielded the overall accuracy result of 83.2%. This study also highlighted that PKS gasification produced 53.74% and 90.51% higher composition of H_2 and CO respectively as compared to coal gasification. Whereas coal gasification produced 81.35%, 71.31% and 52.29% higher composition of CH_4, H_2O and CO_2 respectively as compared to PKS gasification. Hence, PKS produced 66.2% higher combustible gas of H_2 and CO than coal. PKS is thus considered as a potential renewable feedstock for gasification process as an alternative to the non-renewable coal. In addition, PKS gasification produced 52.29% lesser composition of CO_2 as compared to coal gasification.

Keywords: Gasification, downdraft gasifier, Palm Kernel Shell (PKS), coal, Computational Fluid Dynamic (CFD), syngas composition

1. Introduction

Fuel and power generation technologies are commonly designed to use coal as energy source. Coal is a reliable power source that offers predictability. However, as a fossil fuel, coal is not a renewable energy and possesses a finite supply. Coal is also harmful for the environment compared to other forms of energy and power production that humans use today. Coal also contains the most carbon dioxide for every BTU that is produced. According to the Energy Information Administration (EIA), coal with a carbon content of 78% and a heating value of 14,000 BTU would produce

*Corresponding author: afzanizam@uthm.edu.my

about 92.68 kilograms of CO_2 per 1 million BTU when completely combusted [1]. Hence, an alternative fuel is required to substitute coal as a primary source of energy.

Palm oil is an essential product that has improved the scenario of agriculture and economy in Malaysia. Palm kernel shell (PKS), one of the waste products from the palm oil industry, is one of the potential renewable energies. PKS is a solid material with a high carbon content that is currently used as a boiler fuel; however, its combustion efficiency is minimal. PKS can be converted into syngas, a useful form of energy, by using gasification technology [2]. Gasification is a thermochemical process that transforms carbonaceous materials such as biomass into usable fuels or chemicals [3]. The generated syngas can be directly utilized for heating or power generation or as a raw material for chemical feedstock production. Using syngas as a fuel for gas turbines is a common practice and globally well recognized [4].

Computational Fluid Dynamics (CFD) modelling has previously been implemented to analyse the characteristic of biomass gasification as to increase the operational conditions performance of an existing gasifier. CFD is gradually favoured as the primary research technique on biomass gasification due to the high costs of experimental operations and cost-effective options for discovering the various arrangements and operating conditions of gasification reactor at any scale. Analysis of biomass gasification using downdraft method has recently been conducted using CFD simulation approach via multiphase model [7, 8]. The flow regime can be used to govern a suitable multiphase model for the multiphase system. The volume of fluid (VOF) model is utilized for slug and stratified/free surface flows. Slurry flow, hydro transport, bubble, droplet, and particle-laden flows, on the other hand, employ either the mixture model or the Euler model when the phase mix and/or dispersed phase volume fractions exceed 10%. Euler model is used for general and complex multiphase flows that comprise multiple flow regimes, flow aspect and appropriate model selection. The Euler model is the one of the most complex multiphase models in ANSYS Fluent. For each phase, it solves a set of momentum and continuity equations. The pressure and interphase exchange coefficients are used to achieve those coupling set. The way this coupling is handled is determined by the sort of phases involved. Granular (fluid–solid) flows are handled differently than non-regular (fluid–fluid) flows. The properties of granular flows are determined by the use of kinetic theory. The type of mixture being represented is also depend on the amount of momentum exchange between the phases. The equation and employment of the Euler model in the present study are further explained in the methodology section.

Two approaches are widely used for the numerical calculation of multiphase flows: Euler–Lagrange approach and Euler–Euler approach. The present study focused on Euler–Euler approach as done in the previous research by González and Pérez, Kumar and Paul, and Guo et al. [7-9]. The different phases in the Euler–Euler technique are mathematically handled as interpenetrating continua. The concept of the volume fraction is presented since the volume of a phase cannot be occupied by the other phases. The sum of these volume fractions is one, and they are considered to be a continuous function of space and time. In order to obtain a set of equations with a similar structure for all phases, conservation equations for each phase are derived. These equations are solved by delivering constitutive relations derived from empirical data or, in the case of granular flows, by using kinetic theory. [10]. Thus, the model is fit to model flow in a pipe and in an enclosed body where the difference in pressure is small. The present study did not utilize Euler–Lagrange approach because the fluid phase is treated as a continuum by solving the time-averaged Navier–Stokes equations, while the dispersed phase is solved by tracking a large number of particles, bubbles, or droplets through the calculated flow field [11]. The momentum, mass, and energy are interchangeable between the dispersed phase and the fluid phase. The particle or droplet trajectories are computed individually at specific intervals for the fluid phase calculation. Therefore, the model is appropriate to model the process of spray dryers, coal and liquid fuel combustion, and some particle-laden flows, but inappropriate to model liquid–liquid mixtures [11].

The performance of biomass gasification using downdraft method via CFD simulation analysis and Euler–Euler approach has been previously investigated in a few studies. Fortunato et al. [12] used Euler−Euler approach to model the downdraft gasification of saw dust. The results show that the model is able to assess, with a fairly good agreement, both the composition and the heating value of the syngas with experimental results. Ostermeier et al. [13] used Euler–Lagrange approach to model the gasification of wood pellets in a downdraft gasifier. The result shows that the model is capable to predict the gas composition and temperature distribution in the gasification process. Kumar and Paul [8] also used Euler–Lagrange approach for rubber wood gasification, and the results also show a good agreement with experimental results. González and Pérez [7] used Euler–Euler model to characterize the downdraft gasification of leaf pellets. The study reported that the convective heat transfer from gas to solid phase was increased as the airflow increased.

The implementation of renewable energy from biomass for gasification process pose significant challenge towards the usage as an alternative fuel for coal which is non-renewable as to meet the performance requirement in producing high syngas quality. Hence, it is essential to analyse the reaction mechanism behaviour between zones in the gasifier for both coal and biomass feedstock as to examine the capability in producing higher combustible gaseous in syngas. Based on previous studies, computational simulation analysis of gasification using oil palm-based waste is rarely investigated. Hence, fundamental understanding on the performance of gasification using palm waste has not been thoroughly discussed. This present study aims to compare and analyze the downdraft gasification characteristics between coal and palm kernel shell (PKS) biomass using CFD simulation. The effect of those feedstocks on the production of reactive element in syngas was evaluated based on the critical analysis of reaction during gasification process.

2. Material and Method

2.1 Transport Equation for Standard K-E

The realizable k-ε model was adapted from González and Pérez (2019) and employed in the present study to simulate the turbulent flow as in Equation 1 and Equation 2. The turbulence model considerations were depending on the physics encompassed in the flow, the known practice for a certain type of issue, the level of precision necessary, the available computer resources, and the length of time available for the simulation. The present study was using the turbulence model from González and Pérez base on the justification of the similar operational gasification reactor and feedstock from biomass which relatively demonstrate an identified flow concept of physics. In addition, some initial studies showed that the realizable model offers higher performance of all the k-ε model versions for several validations of separated flows and flows with complex secondary flow features including flows that involving rotation, boundary layers under strong adverse pressure gradients, separation, and recirculation. L.C.B.S. Reis et. al. numerically modeling the turbulent heating reaction in the reactor and reported that Realizable k-ε models which account for the effects of swirl have greater potential to predict more accurate predictions for swirling flows [14].

For turbulence kinetic energy (k):

$$\frac{\partial}{\partial t}(pk) + \frac{\partial}{\partial x_i}(pku_i) = \frac{\partial}{\partial x_j}\left[\left(\mu + \frac{\mu_t}{\sigma_k}\right)\frac{\partial k}{\partial x_j}\right] + P_k + P_b - \rho\varepsilon - Y_M + S_k \tag{1}$$

For dissipation of ϵ:

$$\frac{\partial}{\partial t}(p\epsilon) + \frac{\partial}{\partial x_i}(p\epsilon u_i) = \frac{\partial}{\partial x_j}\left[\left(\mu + \frac{\mu_t}{\sigma_\epsilon}\right)\frac{\partial k}{\partial x_j}\right] + C_{1\epsilon}\frac{\epsilon}{k}(P_k + C_{3\epsilon}P_b) - C_{2\epsilon}\rho\frac{\epsilon^2}{k} + S_\epsilon \tag{2}$$

where the turbulent viscosity is modelled as

$$\begin{aligned} \mu_t &= \rho C_\mu \frac{k^2}{\epsilon} \\ P_k &= -\overline{\rho u'_i u'_j}\frac{\partial u_j}{\partial x_i} \\ P_k &= \mu_t S^2 \end{aligned} \tag{3}$$

where S is the modulus of the mean rate-of-strain tensor, defined as

$$\begin{aligned} S &= \sqrt{2S_{ij}S_{ij}} \\ P_b &= \beta g_i \frac{\mu_t}{Pr_t}\frac{\partial T}{\partial x_i} \end{aligned} \tag{4}$$

where Pr_t is the turbulent Prandtl number for energy and g_i is the component of the gravitational vector in the y-axis direction. For realizable k-ε models, the default value of Pr_t is 0.85. The coefficient of thermal expansion, β, is defined as

$$\beta = -\frac{1}{\rho}\left(\frac{\partial p}{\partial T}\right)_P \tag{5}$$

The model constants $C_{1\epsilon}$, $C_{2\epsilon}$, $C_{3\epsilon}$, σ_k, C_μ, and σ_ϵ were established to ensure that the model performs well in this simulation. The model constants are as stated:

$$C_{1\epsilon} = 1.44,\ C_{2\epsilon} = 1.92,\ C_{3\epsilon} = -0.33,\ \sigma_k = 1.0,\ C_\mu = 0.09,\ \sigma_\epsilon = 1.3 \tag{6}$$

The realizable k-ε model was adapted because it is fit to model free-shear layer flows with relatively small pressure gradients. Realizable k-ε turbulence model was used because it performs great with confined flow, straight boundary layers, and straight flow. ANSYS employs realizable k-ε turbulence model to validate turbulence model during the gasification process. The realizable k-ε turbulence model also improves the prediction over mean flow for complex

structure. ANSYS Fluent defines modeled transport equations for kinetic energy (k) and rate of dissipation (ε) as in Equation 7 and Equation 8, respectively.

$$\frac{\partial}{\partial x_j}\left[\left(\mu+\frac{\mu_t}{\sigma_k}\right)\frac{\partial k}{\partial x_j}\right]+G_k+G_b-Y_M+S_k \tag{7}$$

$$\frac{\partial}{\partial x_j}\left[\left(\mu+\frac{\mu_t}{\sigma_k}\right)\frac{\partial k}{\partial x_j}\right]+\rho C_1 S_\varepsilon-\rho C_2\frac{\varepsilon^{\,2}}{k+\sqrt{v\varepsilon}}+C_1 G_b+S_E \tag{8}$$

Where

$$C_1=\left(0.43\frac{\eta}{\eta+5}\right)$$
$$\eta=\sqrt{S} \tag{9}$$
$$S=\sqrt{2S_{ij}S_{ij}}$$

S_{ij} = velocity of material
ij = no. of material

The model constants $C_1\varepsilon$, C_2, σ_k, and σ_ε were established to ensure that the model performs well for certain canonical flows. The model constants are as follows:

$$C_1\varepsilon = 1.44,\ C_2 = 1.9,\ \sigma_k, = 1.0,\ \sigma_\varepsilon = 1.2 \tag{10}$$

2.2 Euler Model

The present study implemented the Euler multiphase model to solve a set of n momentum and continuity equations for each phase. Through the pressure and interphase exchange coefficients, the coupling is achieved. The equations for Euler multiphase flow model, as solved by ANSYS Fluent, are presented in Equation 11:

$$\frac{1}{\rho_{rq}}\left(\frac{\partial}{\partial t}\left(\alpha_q\rho_q\right)+\nabla\left(\alpha_q\rho_q\underset{V}{\rightarrow}_q\right)=\sum_{p=1}^{n}\left(\dot{m}_{pq}-\dot{m}_{qp}\right)\right) \tag{11}$$

where ρ_{rq} is the phase reference density or the volume-averaged density of the q[th] phase in the solution domain. The solution of this equation for each secondary phase is sum up along with the condition of the volume fractions. This allows for the calculation of the primary phase volume fraction of the species [9].

2.3 Grid Setup

The 3D gasifier model was constructed and meshed in ANSYS Mesh, a commercial meshing software. As this study mainly focused on the simulation flow in the fluid domain of the gasifier, the geometry was meshed for the fluid domain of the gasifier and the solid domain was suppressed in ANSYS Space Claim. The gasifier had a diameter of 2.68 m and it was meshed in predominantly tetrahedron cell shapes, as shown in Fig. 1. Tetrahedron mesh that yields better and more accurate results can appropriately fit complex geometry. In addition, the computational cost for tetrahedral elements is lower because there is no unnecessary numerical integration [18].

The present study used proximity and curvature as the size function for the meshing process. The maximum face size was set to 0.146 m and the maximum tetrahedron size was set to 0.29118 m. This study also used inflation on the model with the transition ratio set to 0.272 and a growth rate of 1.2. After the mesh had been generated, the model contained 58439 nodes and 165626 elements with a skewness of 0.783. One of the primary quality measurements for a mesh is skewness. A skewness value of 0 indicates an equilateral cell (best) and a value of 1 indicates a completely degenerate cell (worst). Highly skewed faces and cells below the skewness of 0.7 are unacceptable because the equations being solved assume that the cells are relatively equilateral or equiangular [19].

2.4 Grid Setup

The Four major steps were performed in this study: geometry development, geometry mesh, Fluent simulation setup, and data extraction. The first step of the simulation process was to model the fixed bed downdraft gasifier using

Solidworks software package as illustrated in Fig. 2. The design parameters of the simulation to model the gasification process were adapted from the previous research conducted by Liu et al. which also using Euler-Euler multiphase model [15]. The geometry design of the reactor which critically focused on the oxidation zone design or throated area were adapted from the Handbook of Biomass Downdraft Gasifier Engine System [20].

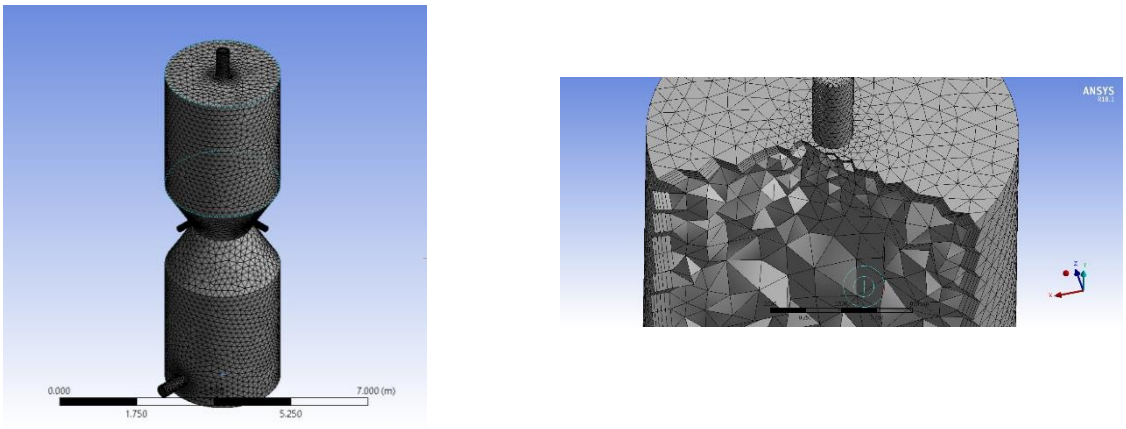

Fig. 1 - The generated mesh model and its cross-sectional view

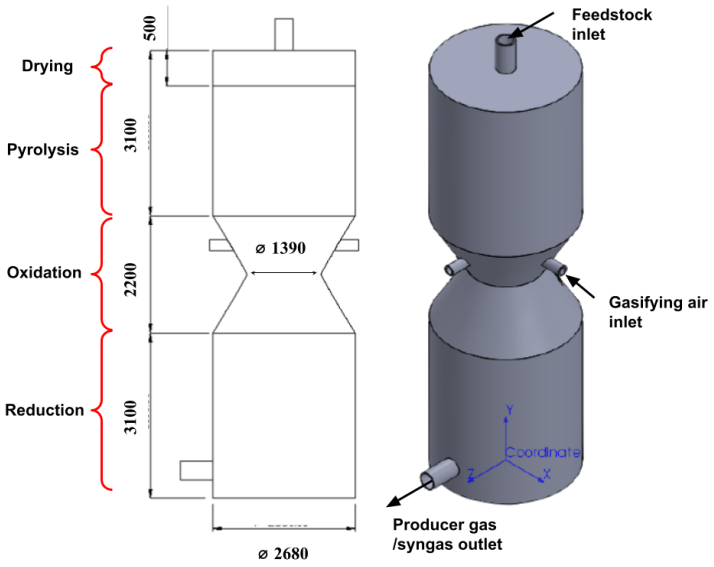

Fig. 2 - Fixed bed downdraft gasifier 3D model

Table 1 - Biomass parameters

Type of analysis	Parameter	Type of biomass	
		Coal (wt %)	PKS (wt %)
	Reference	[12]	[14]
Ultimate	Nitrogen	1.00	3.57
	Carbon	85.00	44.29
	Hydrogen	10.00	9.01
	Oxygen	4.00	43.13
Proximate	Ash	10.00	11.75
	Volatile Matter	50.00	62.82
	Fixed Carbon	30.00	19.10
	Moisture Content	10.00	6.33

The model was defined as a poly solid in ANSYS workbench. The model was meshed using ANSYS Mesh with the forms of tetrahedron cells prior to the model simulation conditional setup process in the ANSYS Fluent environment. The gravitational force was set to act on the y-axis at 9.81 m/s^2. The solver preferences were then established in Fluent. k-ε turbulence model was established with possible near-wall treatment. The species model was set to non-premix combustion, and the fuel for the gasification was defined by using the proximate and ultimate analyses as shown in Table 1. The ultimate and proximate analyses were performed using the properties presented by Liu et al. and Ahmad et al., who also used coal and PKS as feedstock, respectively [18,20]. The fixed carbon content for coal was higher than PKS. Hence the tendency of coal to produce higher combustible gas from the component of carbon is higher. However, the moisture content (which reduce the formation of carbon component) for PKS was lower compared to coal. Thus, detail analysis of gasification mechanism process is vital to compare the capability of coal and PKS in producing higher combustible syngas. The boundary of the simulation was set to fluid, and the operating boundary condition for the model such as pressure was defined at 101.3 kPa. The inlet mass flow rate and temperature for the gasification fuel (coal) were set at 30 kg/s and 400 K, respectively. Meanwhile, the mass flow rate and temperature for the gasification agent (air) were set to 109 kg/s and 900 K, respectively. All the simulation parameters are tabulated in Table 2. During the simulation, the mole fraction for every syngas species produced during the gasification process was monitored by the console for convergence. The convergence criteria were set to 10^{-6} in the units of mole fraction for every syngas species produced during the gasification process. The simulation was initialized using hybrid initialization before it was run. Hybrid initialization solves the Laplace equation to produce a velocity field that conforms to complex domain geometries, and a pressure field which smoothly connects high- and low-pressure values in the computational domain. Surface integral and the x-y plot were utilized to extract syngas composition, temperature, pressure, and velocity data for both gasification simulations after the calculation was completed. The syngas species contour was generated for analysis and discussion.

3. Results and Discussion

The coal simulation was analyzed and used as a baseline. The coal simulation results were validated with the results from previous studies. The validation process is important to ensure the simulation model produces results with high accuracy. The simulation parameters shown in Table 2 were used for the analysis. Non-premix combustion was utilized as the species model for the Fluent simulation. The convergence criteria were set to 0.000001. The mole fraction of the syngas composition was carefully observed for both simulations (coal and PKS) in each iteration process. The mole fraction of the species was rounded to six decimal places. The mass flowrate was set to ensure the mass balance is achieved during the simulation process. The result was validated with 83.2% overall accuracy for the gasification of coal. The simulation analysis was then repeated using PKS as feedstock fuel.

Table 2 - Simulation Parameters

Parameters	Value/Items	Reference
Gasifier Type & Parameters	Fixed Bed Downdraft Gasifier	[20]
Turbulence model	Realizable k-ε	[7-9]
Approach	Euler–Euler	[7-9]
Gasifier Temperature	900 K	[20]
Gasifier Pressure	1 atm	[20]
Gasifier Agent	Air	[20]
Gasifier Agent Flowrate	109 kg/h	[20]
Biomass Feed Rate	30 kg/h	[20]

3.1 Results Validation

The product gas composition from the gasification process was identified based on the syngas composition, which consists of carbon monoxide (CO), hydrogen (H_2), carbon dioxide (CO_2), methane (CH_4), and nitrogen (N_2). A robust simulation model is expected to yield identical results to those from previous studies that used similar process parameters and gasification fuel chemical compositions. Hence, the present model was validated before continuing with the simulation study using different feedstock types. The results of the present study were then compared with those from a previous study as shown in Fig. 3 with the compositional units of mole fraction. The error was calculated by using Equation 6.

$$Error\% = \frac{|Mole\ Fraction_{Simulation} - Mole\ Fraction_{Previous\ Study}|}{Mole\ Fraction_{Previous\ Study}} \times 100\ \% \quad (12)$$

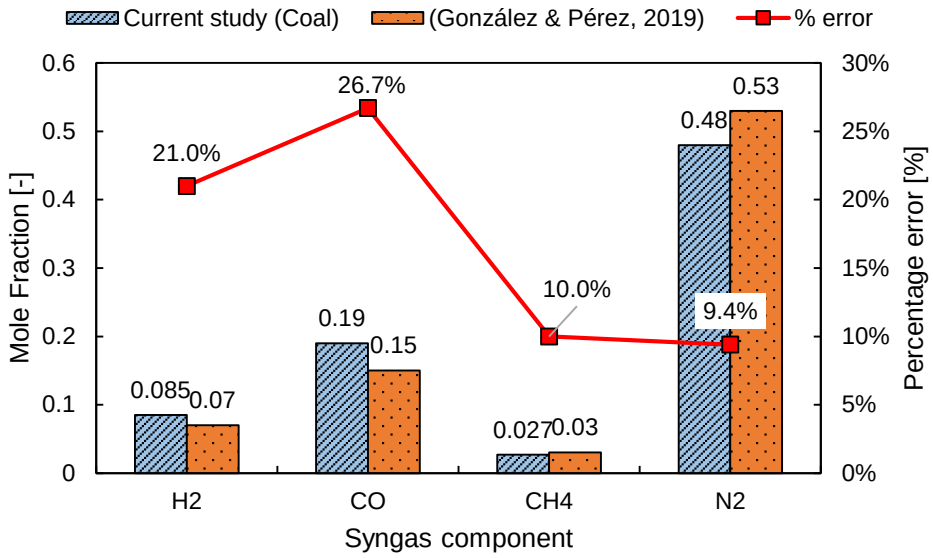

Fig. 3 - Result comparison between the present study with the previous study (Gonzalez & Perez, 2019) [5]

Under the same process parameters and fuel as shown in Table 2, the overall error of the simulation was 16.68%. The error of the simulation prediction for H_2 was 21.66%, while CO error prediction value was 26.75%. The composition of CH_4 was predicted with an error of 9.15%, whereas the error of inert N_2 gas prediction was 9.17%. Data comparison with a previous study carried out by Gonzalez and Perez reveals a good agreement with the present study, in which all the error values were lower than 27% for every species of syngas produced. The deviation of the values between both results was caused by the different species model used in the simulation process. The present study utilized non-premix combustion for the simulation process while Gonzalez and Perez did not specify the species transport model used in their study [7]. This may have caused the gasification model to produce variations in the syngas composition between both simulations.

3.2 Gasification Characteristics of Coal

Surface integral was utilized in this study to obtain the product gas composition produced at the gasifier outlet. From the simulation, coal did not exhibit decomposition process at the drying zone as no significant reactive syngas component for H_2 and CO was produced in that area, as shown in Fig. 4. Drying zone process occurred as the moisture content in biomass began to be removed before it entered the pyrolysis zone. The presence of H_2 and CO was typically higher at oxidation and reduction zone area. Hence, gasification of coal produced higher concentration of H_2 and CO at the reactor exit. According to Maya et. al. [6], the high temperature medium in oxidation zone involved the exothermic and endothermic reactions of gasification fluids and products respectively. Hence, the production of H_2 was promoted by higher temperature as the process involved the primary water-gas reaction and steam-methane reform. The high concentration of CH_4 particularly at pyrolysis zone but reduce at reduction zone as the gas pass through the oxidation zone. This was due to the reforming of CH_4 with H_2O via endothermic reactions which taking place in pyrolysis zone. Thus, gasification of coal caused the production of CH_4 at the reactor exit was lower. This primary observation on the distribution of gaseous component in reactor can become a critical understanding database in determining the reaction behavior within the reactor if coal is used as feedstock.

Fig. 5 showed that all of the water in coal was vaporized completely where H_2O is mainly concentrated at pyrolysis zone. Syngas started to appear during the gasification process in that pyrolysis zone due to the thermal decomposition of coal. The energy required for the thermal composition was generated from the oxidation [21]. Coal began to decompose with heat as its temperature increased above 500 K in the pyrolysis zone. Coal was broken down into a combination of solid, liquid, and gas. The solid that remained unreacted is known as gasification char. Gasification char is the finer component of the gasifier solid residuals which is made up of unreacted carbon and varying proportions of siliceous ash [14]. The gas and liquid released by the gasification process are called syngas and tar, respectively [21]. The gas and liquid produced during pyrolysis were coal fragments that had broken down with heat. These fragments are the more complicated H, C, and O molecules in the coal that are commonly referred to as volatiles [21].

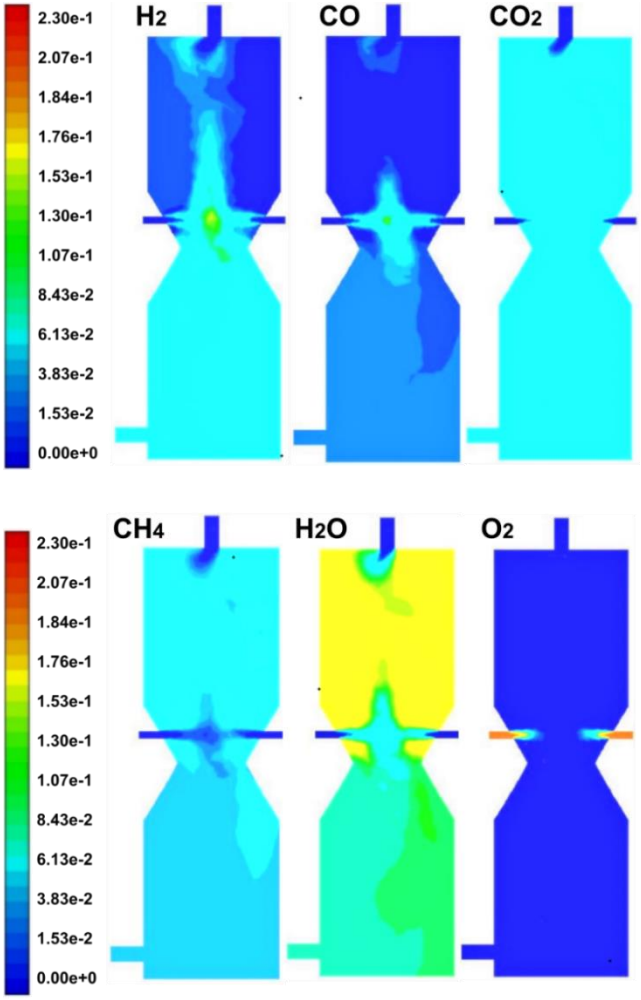

Fig. 4 - Contour of H_2, CO, CO_2, CH_4, H_2O, and O_2 for coal gasification

At the oxidation zone, the gasification agent (air) was injected to react with the products of the pyrolysis zone, to provide heat energy for the gasification process. This reaction took place between 700 and 1000 K. The volatile matter from the pyrolysis zone was also subjected to the combustion process to generate heat for reduction reaction, in which the CO_2 and H_2O concentrations were reduced. The pressure, temperature, and velocity of the gasifier increased rapidly in the oxidation zone due to the introduction of the gasification agent.

In the reduction zone, four major reactions with limited O_2 supply took place: water–gas reaction, water shift reaction, Boudouard reaction, and methanation [16]. Reduction in a gasification process was accomplished by introducing carbon dioxide (CO_2) or water vapor (H_2O) to the volatiles of coal. The carbon volatiles in the coal were highly reactive with oxygen. The high volatility was attributed with the reaction of radical O atom from the water vapor and carbon dioxide. Hence, there are more available radical O and C atoms during this process [15]. This reaction took place with the temperature ranging from 700 to 800 K. The oxygen element is also more prone to bond with the radical C atom than to its own component [15]. Thus, the presence of free radical O atom was insignificant for typical diatomic O_2 form. After the radical O atom had completely reacted, the reduction process was completed [16]. Through this process, CO_2 was reduced by carbon to produce two CO molecules, and H_2O was reduced by carbon to produce H_2 and CO. Both H_2 and CO are combustible fuel gases, and those fuel gasses were then emitted at the outlet of the gasifier and channeled to the desired application.

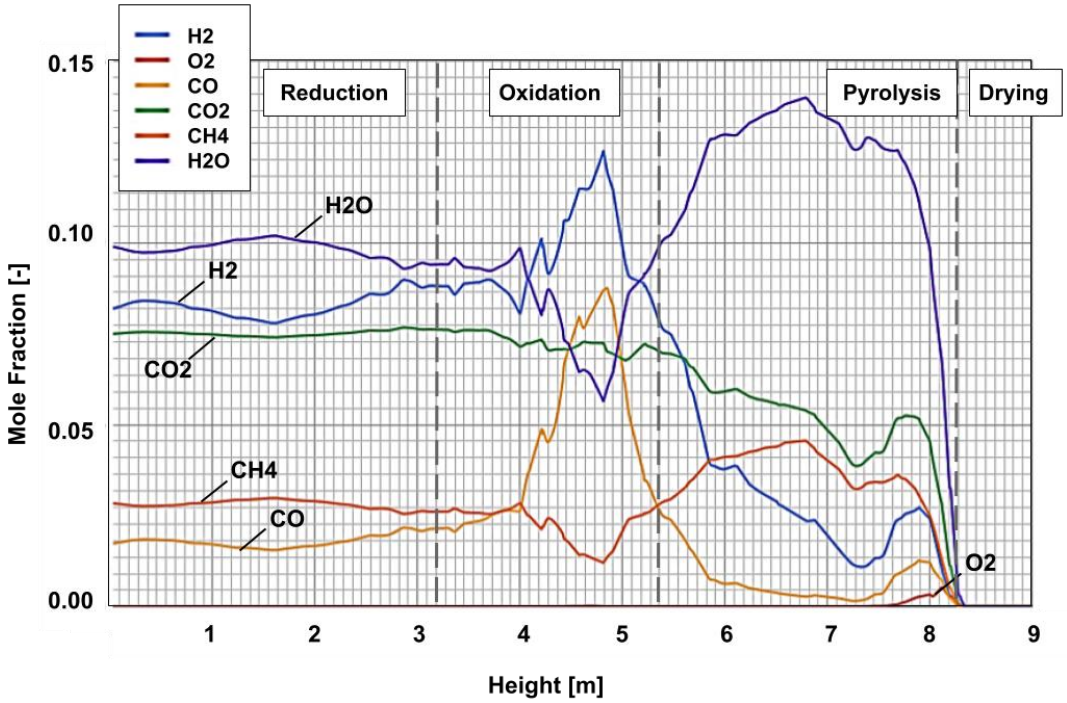

Fig. 5 - The plot of syngas composition against gasifier height

3.3 Gasification Characteristics of PKS

At the pyrolysis zone, all of the water in PKS was vaporized completely. In this study, the H_2O mole fraction in PKS gasification was lower than that of the coal, as shown in Fig. 8. This is due to low moisture content of PKS as compared to coal. PKS began the irreversible devolatilization reaction as the thermal decomposition took place. This is due to the increase of temperature, which was indicated by the higher concentration of CO and H_2 at the pyrolysis zone as shown in Fig. 6. The heat energy required for the thermal composition was acquired from the oxidation zone. PKS began to rapidly decompose with heat and released syngas as its temperature increased above 950 K. The gasses and liquids produced during PKS pyrolysis are PKS fragments that had broken off with heat. These fragments are the more complicated H, C, and O molecules in the PKS that are also typically referred to as volatiles [15]. Fig. 6 also shows that the contour for H_2O is less covered with the yellowish region for PKS compared to coal, which indicates that the amount of H_2O was lower. This corresponds to the higher production of reactive components of H_2 and CO by PKS compared to coal.

At the oxidation zone, the gasification agent (air) was injected to react with the products of the pyrolysis zone to provide heat energy for the gasification process. The oxidation of PKS occurred at higher temperature than the oxidation of coal. The volatile passing through the drying and pyrolysis zone to remove moisture and experience vaporization process. The volatile was then exhibited oxidation process in oxidation zone to produce more gaseous product and finally reduction process to form syngas via the gasification completion process [17]. The combustion process also provided heat energy for CO_2 and H_2O formation in the reduction zone. PKS volatiles also reacted with air to produce carbon dioxide and steam in this particular zone. This is shown in Fig. 7, where the mole fraction of CO_2 and H_2O increased at the oxidation zone. The pressure and velocity of the species in the gasifier increased due to the introduction of the gasification agent at the oxidation zone.

The reduction zone for the gasification of PKS was also attributed with the water–gas reaction, water shift reaction, Boudouard reaction, and methanation [16]. The carbon volatiles in PKS were also highly reactive with oxygen. The high oxygen concentration was favored to react with the radical O atom released from the water vapor and carbon dioxide. This reaction took place within the temperature range from 1000 to 1100 K. The released radical O atom from the bonding promoted the production of CO and H_2 from the CO_2 and H_2O.

3.4 Comparison Between Various Feedstocks

Based on the simulation, PKS produced 52.29% lower CO_2 than coal as shown in Fig. 8. This is due to the complete reaction of carbon volatiles in PKS to form CO during the reduction process. Meanwhile, the carbon volatiles in coal did not completely react due to the high concentration of O_2 in its chemical properties (Ultimate Analysis), as previously indicated in Table 1. This caused the unreacted CO_2 to be discharged at the outlet of the gasifier and led to the higher production of CO_2 by coal than the one produced by PKS.

During the biomass oxidation, PKS produced more CO_2 compared to coal, as shown in Fig. 8. CO_2 reacted completely with oxygen in PKS at the reduction zone to form CO, whereas coal carbon volatiles did not react completely with oxygen due to the limited supply of O atom in its chemical properties. This caused the PKS to produce 90.51% higher CO content than coal. PKS has the advantage over the coal due to its high concentration of volatile oxygen in its chemical properties.

PKS also produced 53.74% higher H_2 content than coal. This is due to the higher concentration of CO in PKS that underwent water shift reaction with H_2O to produce H_2 and CO_2. Although coal contains higher concentration of carbon volatiles than PKS, the limited amount of volatile oxygen hinders the CO_2 production during coal oxidation, thus affecting the process of water–gas, water shift, and Boudouard reactions in the production of H_2 and CO. This caused the reactant of those reactions, which is generally H_2O, to be left unreacted and emitted to the surrounding. Hence, this leads to the higher production of H_2O by coal (71.31%) compared to PKS.

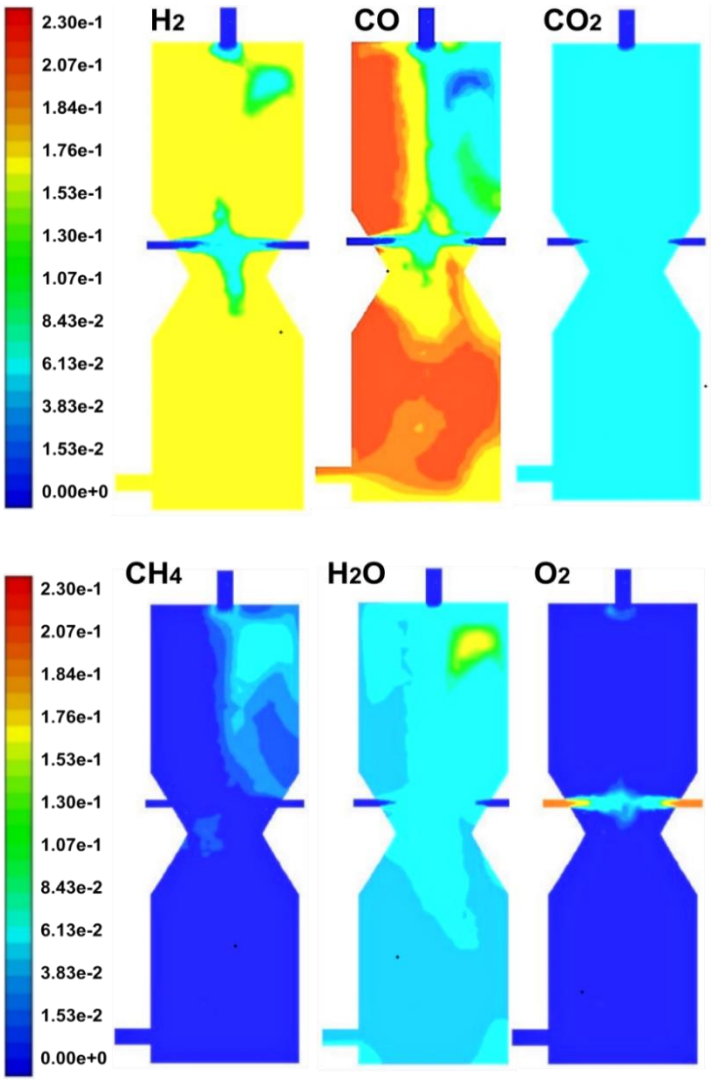

Fig. 6 - Contour of H_2, CO, CO_2, CH_4, H_2O, and O_2 for PKS gasification

Coal produced 81.35% higher CH_4 than PKS. This is due to the higher concentration of carbon molecule in coal than PKS that caused the methanation reaction with H_2 to occur and produce CH_4. This study concludes that PKS gasification produced 53.74% and 90.51% higher H_2 and CO than coal, respectively, when both simulations used similar gasification parameters. Meanwhile, coal gasification produced 81.35%, 71.31%, and 52.29% higher CH_4, H_2O, and CO_2, respectively compared to PKS, as shown in Fig. 8. Thus, gasification of biomass is observed to be a potential candidate for alternative fuel to coal as the combustible gaseous produced was higher based on the simulation analysis. This fundamental understanding can become a vital database for future work especially when involving a justification with experimental work.

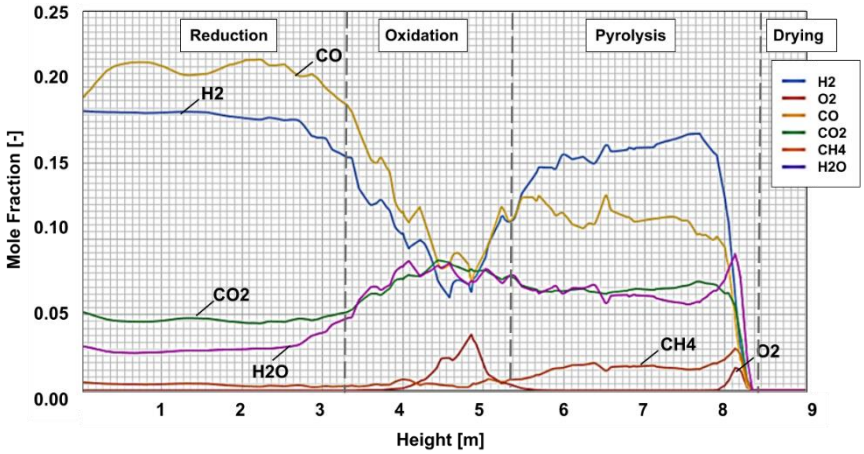

Fig. 7 - The plot of syngas composition for PKS against gasifier height

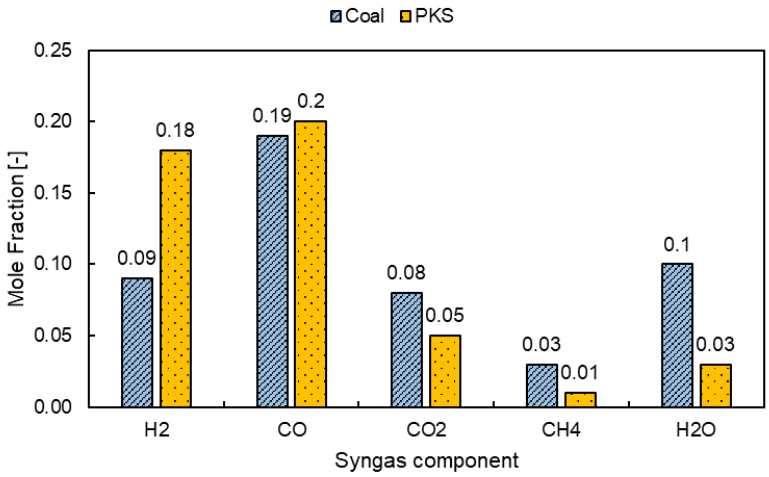

Fig. 8 - The x-y plot for comparison of syngas composition between coal and PKS

4. Conclusion

The present study investigated the effect of different gasification feedstocks on the produced syngas composition via CFD simulation method. The simulation model of gasification using coal as feedstock, and the results of syngas composition were validated with a previous study, which also used coal and similar parameters. The results are in a good agreement as the present model produced a result with an overall accuracy of 83.2% when compared to the previous study. The validated model was then applied for the gasification simulation using PKS as feedstock. The simulation showed that the gasification of coal and PKS were applicable to be modeled to produce the required syngas composition that consists of CO, H_2, CO2, CH_4, H_2O, and N_2. The difference of syngas composition produced by coal and PKS is attributed to the chemical properties of the fuel. The study found that the PKS gasification produced 53.74% higher H_2 and 90.51% higher CO than coal with same conditional parameter setup. In addition, coal gasification produced 81.35% higher CH_4, 71.31% higher H_2O, and 52.29% higher CO_2 than PKS. The future work might be focused on the usage of different gasification agent such as steam, pure O_2 and supercritical water to enhance the production of syngas. Detail of reaction kinetic modelling in the simulation model also vital for accuracy and finally validation with experimental work is a must for authenticity of the study. The use of alternative resources from the biomass waste for gasification as proposed in this work can be one of the potential technologies towards the renewable energy usage. This is due to the capability of PKS biomass in producing higher combustible gases compared to coal. The innovation also demonstrated on the higher amount of H_2 content in syngas produced by PKS biomass. High H_2 syngas is favorable for cleaner combustion technology with higher calorific value and hence comparable with conventional fossil fuel contained energy. Thus, this alternative fuel can become a potential high-performance fuel for combustion technology specifically in power generation system such as gas turbine, boiler, furnace and etc.

Acknowledgement

The authors are grateful to the Universiti Tun Hussein Onn Malaysia (UTHM) for sponsoring this study.

References

[1] MacKinnon, A.J., Duinker, P.N., & Walker T.R. (2018). The application of science in environmental impact assessment (1st ed.). Taylor & Francis Group

[2] Asadullah, M., Ab Rasid, N. S., Kadir, S. A., & Azdarpour, A. (2013). Production and detailed characterization of bio-oil from fast pyrolysis of palm kernel shell. Journal of Biomass and Bioenergy, 316-324. https://doi.org/10.1016/j.biombioe.2013.08.037

[3] Sikarwar, V. S., & Zhao, M. (2017). Biomass Gasification. Elsevier Inc., 205-206. https://doi.org/10.1016/B978-0-12-409548-9.10533-0

[4] Gumz, W. (1950). Gas Producers and Blast Furnaces. New York: John Wiley & Sons.

[5] Prasertcharoensuka, P., Hernandezb, D. A., Bulla, S. J., & Phana, A. N. (2018). Optimisation of a throat downdraft gasifier for hydrogen production. Biomass and Bioenergy 116 216–226, https://doi.org/10.1016/j.biombioe.2018.06.019

[6] Maya, D.M.Y., Lora, E.E.S., Andrade, R.V., Ratner, A., Angel, J.D.M. (2021). Biomass gasification using mixtures of air, saturated steam, and oxygen in a two-stage downdraft gasifier. Assessment using a CFD modelling approach. Renewable Energy, 177, 1014-1030, https://doi.org/10.1016/j.renene.2021.06.051

[7] González, W. A., & Pérez, J. F. (2019). CFD analysis and characterization of biochar produced via fixed-bed gasification of fallen leaf pellets. Journal of Energy, 185-205. https://doi.org/10.1016/j.energy.2019.115904

[8] Kumar, U., & Paul, M. C. (2019). CFD modelling of biomass gasification with a volatile break-up approach. Chemical Engineering Science, 413-422. https://doi.org/10.1016/j.ces.2018.09.038

[9] Guo, F., Dong, Y., Dong, L., & Guo, C. (2014). Effect of design and operating parameters on the gasification process of biomass in a downdraft fixed bed: An experimental study. Journal of International Journal of Hydrogen Energy, 5625-5633. https://doi.org/10.1016/j.ces.2020.116249

[10] Kumar, A., Kent, E., David, Jone., Milford, & Hanna., A. (2009). Steam–Air fluidized bed gasification of distillers grains: effects of steam to biomass ratio, equivalence ratio and gasification temperature. Journal of Bio Resource Technology, 2062-2068. https://doi.org/10.1016/j.biortech.2008.10.011

[11] Patra, C. (2014). CFD Simulation of Fluidized Bed. National Institute of Technology, Rourkela, 10-15.

[12] Fortunato, B., Brunetti, G., Camporeale, S., Torresi, M., & Fornarelli, F. (2017). Thermodynamic model of a downdraft gasifier. *Energy Conversion and Management*, 281-294.

[13] Ostermeier, P., Fischer, F., Fendt, S., DeYoung, S., & Spliethoff, H. (2019). Coarse-grained CFD-DEM simulation of biomass gasification in a fluidized bed reactor. Fuel, 115790. https://doi.org/10.1016/j.fuel.2019.115790

[14] Reis, L.C.B.S., J.A. Carvalho, Jr., Nascimento, M.A.R., Rodrigues, L.O., Dias, F.L.G., Sobrinho, P.M., Numerical modeling of flow through an industrial burner orifice, Energy 186 (2019) 115904, https://doi.org/10.1016/j.applthermaleng.2014.02.036

[15] Liu, H., Elkamel, A., Lohi, A., & Biglari, M. (2013). Computational fluid dynamics modeling of biomass gasification in downdraft gasifier using the Eulerian-Eulerian approach. Industrial and Engineering Chemistry Research, 18162-18174. https://doi.org/10.1021/ie4024148

[16] Fátima Arroyo Torralvo, Constantino Fernández Pereira and Oriol Font Piqueras. (2017). By-products from the integrated gas combined cycle in IGCC systems, Integrated Gasification Combined Cycle (IGCC) Technologies. Pages 465-494. https://doi.org/10.1016/B978-0-08-100167-7.00014-7

[17] Samiran, N.A., Jaafar, M.N.M., Ng, Johan, Lam, S.S., Chong, C.T., Progress in biomass gasification technique – With focus on Malaysian palm biomass for syngas production, Renewable and Sustainable Energy Reviews 62 (2016) 1047–1062, http://dx.doi.org/10.1016/j.rser.2016.04.049

[18] El Marjani, A.Castro Ruiz, F.Rodriguez, M. A., & Parra Santos, M. T. (2008). Numerical modelling in wave energy conversion systems. Journal of Energy. https://doi.org/10.1016/j.energy.2008.02.018

[19] Ahmad, R., Hamidin, N., Ali, U., & Abidin, C. (2014). Characterization of bio-oil from palm kernel shell pyrolysis. Journal of Mechanical Engineering and Sciences, 1134-1140. http://dx.doi.org/10.15282/jmes.7.2014.12.0110

[20] Sikarwar, V. S., & Zhao, M. (2017). Biomass Gasification. Elsevier Inc., 205-206. Solar technical information program;solar energy research institute. U.S. Department of Energy. (2014). Handbook of Biomass Downdraft Gasifier Engine Systems. California: CreateSpace Independent Publishing Platform. https://doi.org/10.1016/B978-0-12-409548-9.10533-0

[21] Patumsawad, S., & Dejtrakulwong, C. (2014). Four zones modeling of the downdraft biomass gasification process: Effects of moisture content and air to fuel ratio. Journal of Energy Procedia, 142-149. https://doi.org/10.1016/j.egypro.2014.07.064